

Processing and mechanical properties of natural rubber/waste-derived nano filler composites compared to macro and micro filler composites



Cindy S. Barrera^a, Katrina Cornish^{a,b,*}

^a Food, Agricultural and Biological Engineering, Ohio Agricultural Research and Development Center, The Ohio State University, Wooster, OH, USA

^b Horticulture and Crop Science, Ohio Agricultural Research and Development Center, The Ohio State University, Wooster, OH, USA

ARTICLE INFO

Keywords:

Natural rubber
Nanocomposites
Waste-derived fillers
Mechanical properties
Processability

ABSTRACT

Nano-sized fillers produced from renewable materials can generate high performance natural rubber (NR) composites while reducing dependency on petroleum. We made NR composites, with both hevea and guayule NR, containing nano-scale waste-derived fillers as complete and partial replacements of carbon black. The effect of nano-filler type and loading on composite mechanical properties was analyzed and compared to previous results with micro and macro fillers. Also, processability of the compounds was investigated. Reinforcement of both NRs was achieved by nano-sized waste-derived fillers, even with complete replacement of carbon black. Increases of up to 2.4 and 1.8 times higher tensile and tear strength, respectively, were achieved in some of the composites compared to the unfilled compound. Better relative reinforcement was obtained in guayule than in hevea rubber due to different rubber macromolecular structure and the strength of the rubber-waste filler interactions. Composites containing waste-derived fillers as co-fillers with carbon black displayed uncommon combinations of properties not achieved with single conventional reinforcing fillers. Furthermore, significant reductions in power consumption during mixing, up to 10% in hevea and 19% in guayule composites, were obtained even by replacement of a small portion of carbon black in the composites. Despite increased interest in nano-sized particles, micro-sized fillers are effective reinforcing fillers when used as partial replacements of carbon black, and can be produced at a much lower cost than nano-sized particles.

1. Introduction

Fillers are extensively used polymer additives, considered essential to attainment of product performance (Leblanc, 2002). Currently the main two commercially used reinforcing fillers are carbon black (CB) and silica. Since the early 1900s, CB has been the most widely used and studied reinforcing filler for rubber composites (Fröhlich et al., 2005; Tohsan and Ikeda, 2014). However, CB is a non-renewable resource derived from petroleum. Furthermore, increased tire production along with reductions in CB production capacity due to increasing environmental regulations in North America and Europe, is likely to lead to CB shortfalls and price rises by 2020 (Moore, 2015; Pourriahi, 2016).

Silica has gained increasing attention as a reinforcing filler since the early 1990s, particularly in the tire industry due to improvements it confers in dynamic-mechanical properties such as lower rolling resistance at equal wear resistance and improved wet grip compared to CB composites (Rattanasom et al., 2007; Stöckelhuber et al., 2010). The use of silica in rubber compounds also has positive impact on the sustainability of the tire industry, due to increased fuel economy and

decreased CO₂ emissions achieved as result of tires' low rolling resistance. Nevertheless, the production of silica requires the use of harsh chemicals and high temperatures (Byers, 2001). Moreover, compounding natural rubber (NR) with silica requires the use of expensive coupling agents to overcome unacceptably strong filler–filler interactions and improve compatibility with NR (Choi et al., 2003; Kato et al., 2014; Murakami et al., 2003). Furthermore, 36% of the silica demand is related to non-rubber products (Notch consulting Inc., 2015), which limits current availability for the rubber industry.

New fillers are desired that can offer similar or better reinforcing and processing properties to CB but be derived from more sustainable sources. Increasingly, research is focusing on the utilization of waste-derived, renewable materials as alternative fillers for elastomers (Abraham et al., 2013; Barrera and Cornish, 2016, 2015; Gopalan Nair and Dufresne, 2003; Intharapat et al., 2013; Ishak and Bakar, 1995; Pasquini et al., 2010; Visakh et al., 2012). This field of research is driven by concerns about environmental footprint, sustainability in manufacturing, and the rising cost of treatment and disposal of high volume waste materials.

* Corresponding author at: Williams Hall, 1680 Madison Avenue, Wooster, OH 44691, USA.
E-mail address: cornish.19@osu.edu (K. Cornish).

Particle size is an important morphological characteristic affecting the utility of alternate fillers as reinforcing agents (Leblanc, 2002). Smaller particles have more surface area per unit weight than bigger particles. Greater surface area facilitates more interfacial contact between the filler and the polymer, which increases the effectiveness of reinforcement (Bandyopadhyay-Ghosh et al., 2015; Szeluga et al., 2015). However, the strength and nature of interactions between the polymer and the filler depends on other filler characteristics such as surface activity (Kohls and Beaucage, 2002). Differences in surface activity result from the presence of chemical groups and structural heterogeneities (Byers, 2001; Fröhlich et al., 2005; Leblanc, 2002), and can be quantified in terms of surface energy of the filler (Cordeiro et al., 2011; Nardin et al., 1990). Big particles ($> 40 \mu\text{m}$) also act as localized stress points, generating flaws within the composite that can initiate failure (Byers, 2001; Samsuri, 2013). Hence, research efforts on alternative filler sources have focused on nano particles for the manufacture of high performance polymer composites (Angellier et al., 2005a; Bitinis et al., 2013; Visakh et al., 2012).

Nevertheless, important drawbacks have been associated with the use of nano particles, including the complexity and high cost of their production compared to macro and micro size particles, and composite processability issues (Abraham et al., 2011; Byers, 2001; Fang et al., 2014; Peddini et al., 2014). The mixing of rubber compounds is a very complex operation. Despite advancements in composites technology, the dispersion of nano particles in the polymer matrix remains a challenge, particularly for non-CB composites. The higher surface area, and active surfaces of these particles, favor interaction between the particles leading to agglomeration that reduces composite performance (Chao and Riggleman, 2013; Donnet and Custodero, 2013; Kueseng and Jacob, 2006). To achieve homogeneous dispersion of nanoparticles in rubber, complex mixes are required that often involve high power consumption, increasing processing costs (Szeluga et al., 2015).

The aim of this study was to evaluate power consumption during mixing of different waste-derived fillers with hevea and guayule rubber, and compare resultant mechanical properties of the nanocomposites to composites made with CB, and micro and macro sized waste-derived particles.

2. Materials and methods

2.1. Materials

Hevea NR (grade SMR-20) and natural rubber latex (NRL, grade Centex), purchased from Centrotech (Chesapeake, Virginia), were used to manufacture hevea rubber composites. Guayule rubber (GNR) was obtained by drying guayule natural rubber latex (GNRL) extracted as described (Cornish, 1996). GNR and GNRL were used to prepare guayule rubber composites. Compounding chemicals, namely zinc oxide, stearic acid, sulfur, the vulcanization accelerator butyl benzothiazole sulfonamide (TBBS), and CB N330 (mean particle size: 108 nm, SD: 31.42 nm), were purchased from HB chemicals (Twinsburg, OH). The waste filler raw materials were generously donated as follows: eggshells (ES) by Michael Foods (Gaylord, MN), carbon fly ash (CFA) by Cargill Salt (Akron, OH), processing tomato peels (TP) by Hirzel Canning Co & Farms (Toledo, OH), and guayule bagasse (GB) was generated as a co-product of latex extraction from shrubs generously donated by PanAridus LLC (Casa Grande AZ).

2.2. Preparation of waste-derived nano-fillers

Raw materials were dried and ground to macro particle size ($300 \mu\text{m} > d > 38 \mu\text{m}$) as described (Barrera and Cornish, 2015). Nano-sized ES, TP and CFA particles were made by wet-milling the macro sized particles using a five liter ball mill, U.S. Stoneware (East Palestine, OH) for 5–8 days. Nano-sized GB particles were prepared by wet-milling with simultaneous hydrolyzation using a sulfuric acid

solution (40%) at room temperature for 2–3 days. The GB dispersion was then centrifuged at 8000 rpm for 10 min using a J2-MC high speed centrifuge, Beckman Coulter (Indianapolis, IN). The solution was decanted and the precipitated particles re-suspended in deionized water. Centrifugation and resuspension was repeated three times to quench hydrolysis.

Aqueous dispersions (1:3 w:v) of each filler were sonicated for 30 min at 35% amplitude using a high intensity ultrasonic processor VCX750, Sonics & Materials (Newtown, CT) to break apart aggregates. Intervals of 10 s on and 5 s off were used to avoid over-heating. Particle size distributions were determined using a Particle size analyzer LA-950V2, Horiba Scientific (Irvine, CA). In addition, primary particle length and width were determined using ImageJ software from TEM micrographs.

2.3. Rubber nanocomposites manufacture

Aqueous filler dispersions were added to latex (NRL or GNRL) (1:1 v:v) under constant mixing using a magnetic stirrer. Latex coagulated during the mixing process was collected and allowed to rest overnight, during which time the rubber exuded most of the entrained water. The samples of coagulated rubber with nano fillers dispersed throughout, were then passed once through a two-roll EEMCO lab mill, roll diameter 15.24 cm and 33.02 cm face width (Rubber City Machinery Corporation, Akron, OH), and dried at 50°C . The resulting materials were used as master batches for compounding with various amounts of unfilled solid rubber (guayule or hevea) and CB to achieve specific waste-derived filler concentrations (5, 10, 20 or 35 phr) (parts per hundred rubber). Total combined filler loading (CB plus waste-derived nano filler) was 35 phr. A standard compounding formulation was used for all the composites (Table 1). Composites containing 35 phr of CB N330 with no other filler were used as reference materials for both NRs, and unfilled compounded rubber was used as a second reference.

CB and compounding ingredients were mixed into the rubber composites through mastication using a Farrel BR lab mixer (Rubber City Machinery Corporation, Akron, OH). The mixing protocol can be summarized in three steps: (1) rubber was added into the mixer and allowed to knead; (2) fillers and stearic acid were added in the mixing chamber. In these two first steps, roto speed was 6.3 rad/s; (3) sulfur and remaining compounding ingredients were added, and rotor speed was increased to 9.4 rad/s. Power required for the mixing of each rubber composite in the lab mixer was recorded using a Pro-server Ex software v 1.3., Pro-face Digital Electronics Corporation (Osaka, Japan). The hot mix was discharged from the mixer, then milled and cured. The processing conditions for rubber compounding and curing were as previously described (Barrera and Cornish, 2015).

2.4. Materials characterization

2.4.1. Mechanical properties

Tensile properties and tear strength were measured according to ASTM D412 and ASTM D624, respectively (ASTM International, 2013a, 2012), along the grain direction at a crosshead speed of 500 mm/min at 23°C . Testing was performed using a tensiometer (Model 3366, Instron,

Table 1
Compounding formulation used to prepare natural rubber composites.

Material	Quantity (phr)				
Natural rubber	100				
Carbon black	35	30	25	15	0
Filler	0	5	10	20	35
Sulfur	3.5				
Zinc Oxide	5				
Butyl benzothiazole sulfonamide (TBBS)	0.75				
Stearic acid	1				

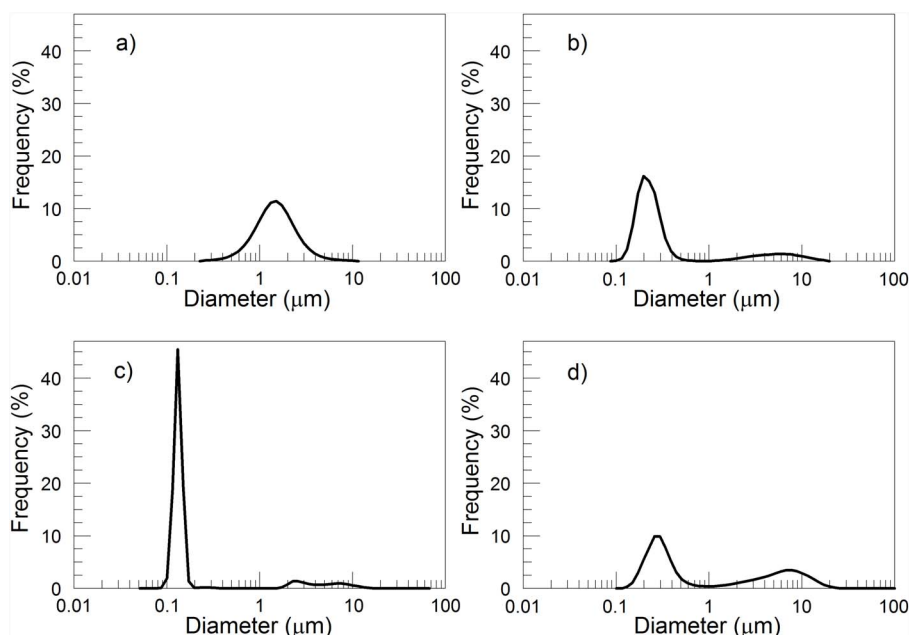


Fig. 1. Nano sized fillers' particle size distribution. (a) Guayule bagasse (median: 1.370 μm , mean: 1.585 μm), (b) carbon fly ash (median: 0.218 μm , mean: 1.109 μm), (c) eggshells (median: 0.125 μm , mean: 0.757 μm), (d) processing tomato peels (median: 0.386 μm , mean: 7.711 μm).

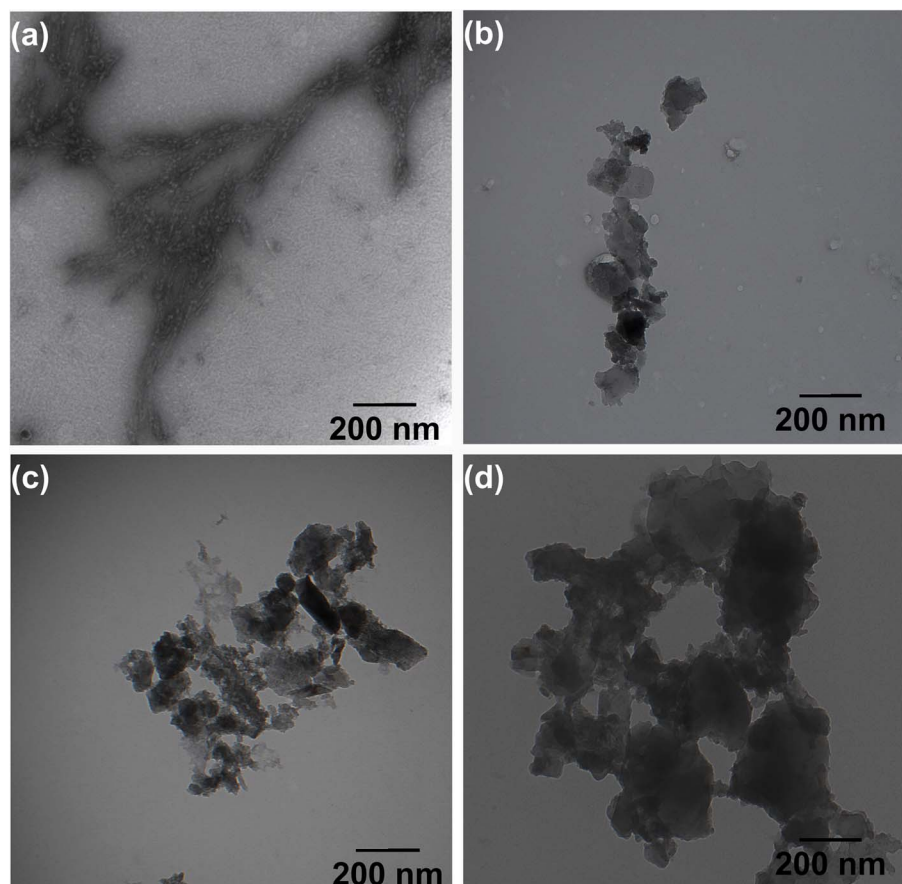


Fig. 2. Transmission electron micrographs of waste-derived filler nano particles. (a) guayule bagasse; (b) carbon fly ash; (c) eggshells; (d) processing tomato peels.

Norwood, MA), with the Bluehill v. 2.26 software package. Five replicates were used for each test. The properties of these composites (300% modulus, tensile strength, elongation at break and tear strength) were compared.

2.4.2. Microscopic analysis

The morphology of the different nano fillers was investigated using a Hitachi H-7500 transmission electron microscope (Tokyo, Japan).

Imaging of the nano particles was done with an accelerating voltage of 80 kV. Aqueous dispersions containing the nano filler were deposited on a copper grid bearing a carbon film and excess liquid was removed by blotting with filter paper. The samples were stained with 2% uranyl acetate solution, blotted with filter paper to remove excess staining solution and allowed to dry.

A Hitachi S-3500N scanning electron microscope (Tokyo, Japan), operated in a high vacuum, was used to investigate the morphology of

Table 2
Waste-derived fillers primary particle length and width.

Filler	Primary particle length (nm)	Primary particle width (nm)	Particle density (g/cm ³)
Guayule bagasse	141.88 ± 46.14	21.01 ± 4.40	1.28 ± 0.39
Carbon fly ash	159.14 ± 64.12	106.99 ± 44.61	1.48 ± 0.27
Eggshells	120.74 ± 57.08	73.83 ± 31.29	2.39 ± 0.67
Processing tomato peels	195.81 ± 82.90	150.89 ± 69.34	1.56 ± 0.19

the different composites at the fracture surface and distribution of the fillers within composites. After tensile testing, cross sections of each composite were cut and washed with 70% aqueous ethanol, to eliminate surface contamination. The samples were sputter-coated with a thin layer of platinum (0.2 KÅ) by an Anatech Hummer 6.2 Sputtering system prior to analysis in order to improve their conductivity, allowed to dry, and imaged.

2.4.3. Swelling test

Crosslinking density was determined based on solvent-swelling measurements. These measurements were performed on samples of 10 mm × 10 mm × 2 mm. The initial weight of the dry samples was recorded to an accuracy of 0.1 mg. Samples were immersed in toluene and kept at 25 °C. The samples were periodically removed from the test bottles, weighed and immediately replaced in the bottles. This procedure was continued until no change in sample weight was noted. The swelling ratio of the samples was calculated as follows:

$$\text{Swelling ratio}(\%) = \frac{(W_t - W_0)}{W_0} * 100$$

where W_0 and W_t are the weights of the samples before and after a time t of immersion, respectively. The value of swelling ratio of each composite was the average of three specimens. Crosslink density of the sample was calculated using the Flory-Rehner equation (ASTM International, 2013b).

$$v_e = \frac{-[\ln(1 - V_r) + V_r + x_1 V_r^2]}{[V_1(V_r^{1/3} - V_r)/2]}$$

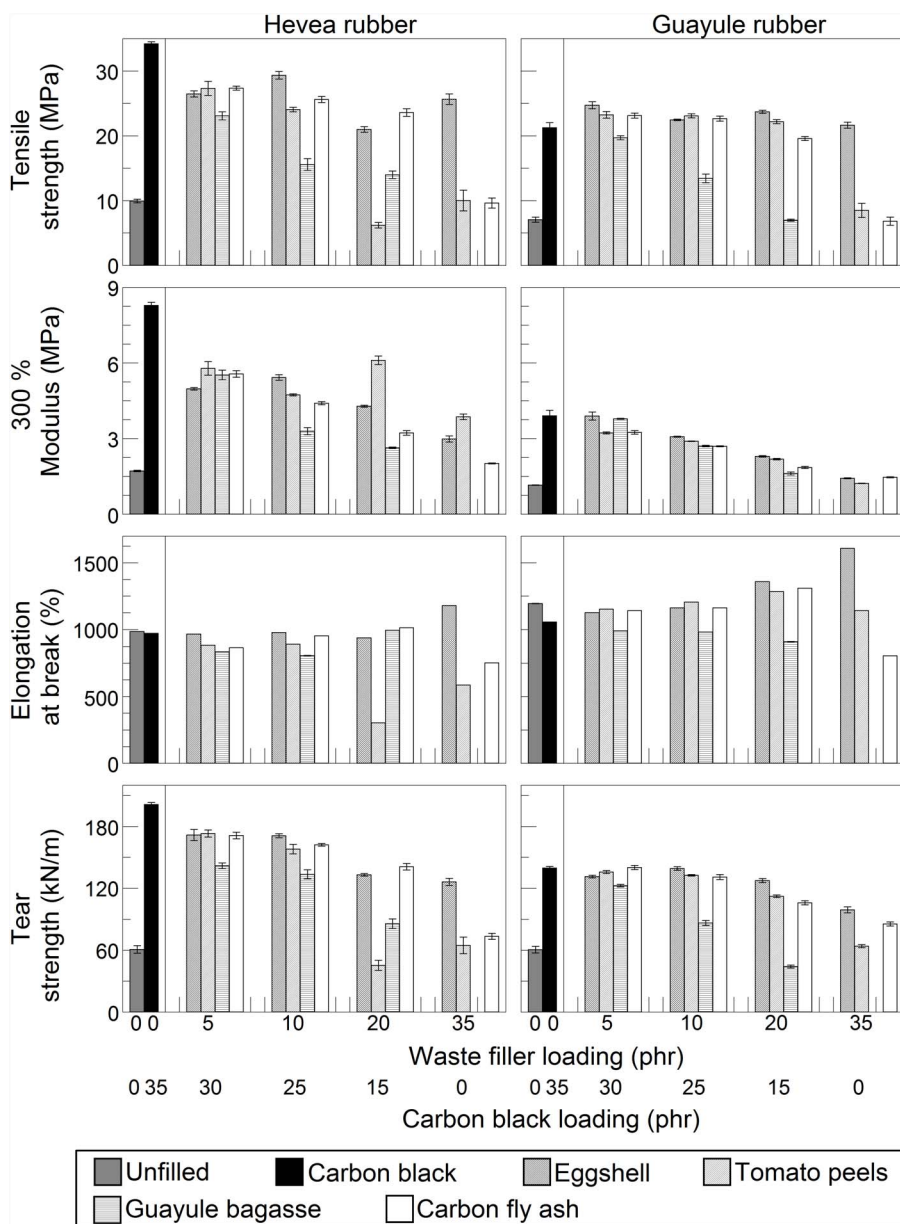


Fig. 3. Mechanical properties of hevea and guayule natural rubber nano composites and unfilled compounds. Total filler (carbon black plus waste-derived filler), in all composites was 35 phr. As the waste filler loading increases the carbon black filler decreases by the same weight amount.

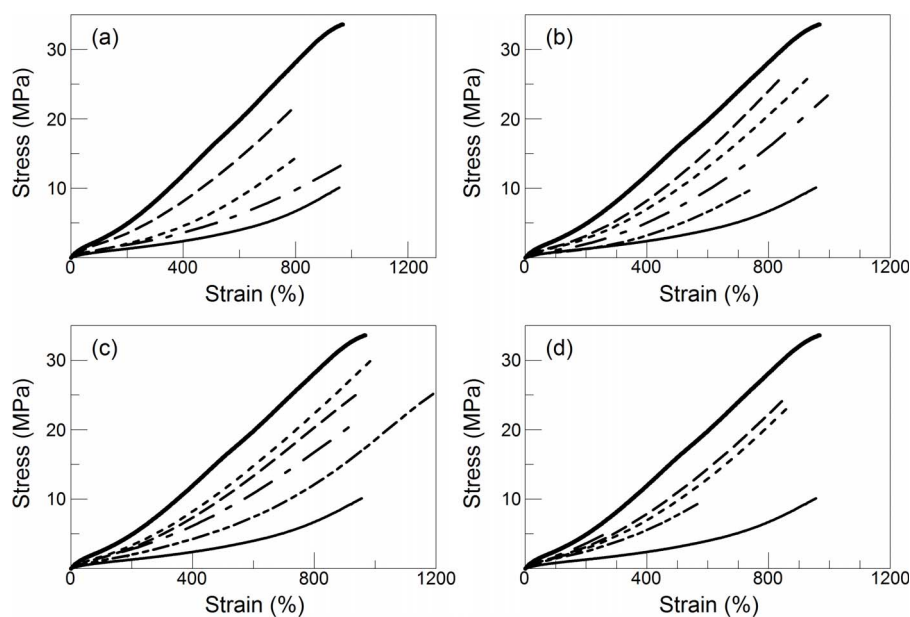


Fig. 4. Stress vs Strain curves of hevea rubber nanocomposites made with (a) guayule bagasse; (b) carbon fly ash; (c) eggshells; (d) processing tomato peels. Total filler loading is 35 phr. As the waste filler loading increases the carbon black filler decreases by the same amount. Waste filler loading: --- 5 phr, 10phr, - . - . 20 phr, - - - 35 phr, — unfilled compound, — 35 phr carbon black.

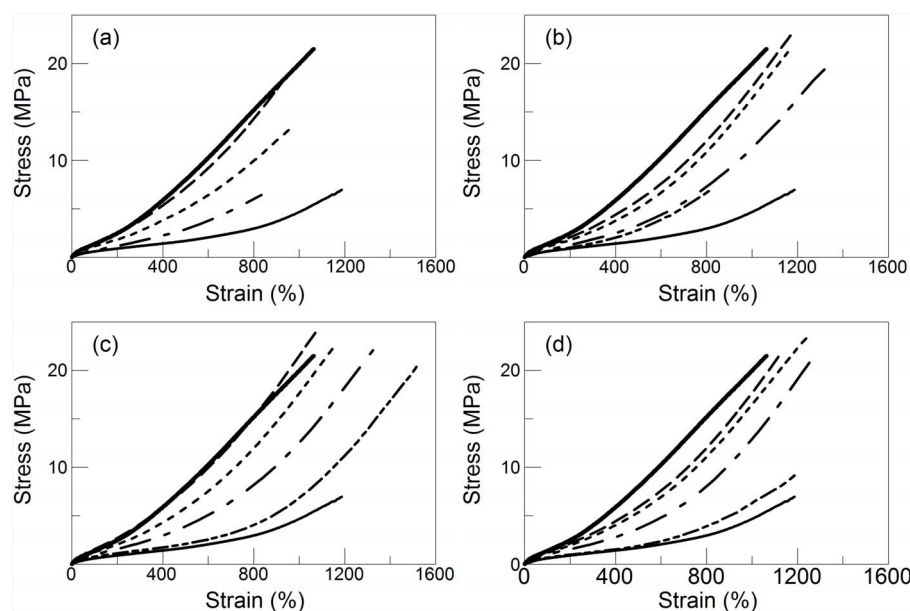


Fig. 5. Stress vs Strain curves of guayule rubber nanocomposites made with (a) guayule bagasse; (b) carbon fly ash; (c) eggshells; (d) processing tomato peels. Total filler loading is 35 phr. As the waste filler loading increases the carbon black filler decreases by the same amount. Waste filler loading: --- 5 phr, 10phr, - . - . 20 phr, - - - 35 phr, — unfilled compound, — 35 phr carbon black.

where x_1 is the polymer-solvent interaction parameter (0.393) and V_1 is the molar volume of the solvent ($106.2 \text{ cm}^3/\text{g mole}$) (Sheehan and Bisio, 1966). V_r is the volume fraction of polymer in a swollen network in equilibrium with solvent, and was calculated as :

$$V_r = \frac{W_r/\rho_r}{W_r/\rho_r + W_s/\rho_s}$$

where W_r and W_s are weights of the dried sample and solvent absorbed by the sample, respectively. ρ_r and ρ_s are the density of the rubber compound and solvent respectively. ρ_r was calculated as described (ASTM International, 2013b).

2.5. Statistical analysis

Cluster analysis was done in order to group composites with similar mechanical properties. The data were standardized so the extent of the contribution of each response variable in the classification was not affected by differences in scale. Cluster analysis was performed using Vegan package (Vegan v. 2.3-0) implemented in R (R Core Team,

2014). Euclidian distance was used to measure the similarity between the treatments. Ward's method was used as the linkage method. Multiple means comparison Tukey-Kramer tests ($p < 0.05$) was used to detect significant differences in the mechanical properties of composites obtained with different formulations.

3. Results

3.1. Filler characterization

Variations in particle size distribution were observed among the different materials (Fig. 1). Nano sized ES particles had the narrowest distribution. Broader distributions and larger mean particle size of the other materials reflected their higher tendency to agglomerate and difficulty in identifying individual particles due to the limitations of the particle sizer instrument. However, all of the waste-derived fillers had elementary particles with nano size dimensions (Fig. 2, Table 2). Variations in particle morphology and particle density were also observed (Fig. 2, Table 2). CFA, ES and TP presented more irregular particle

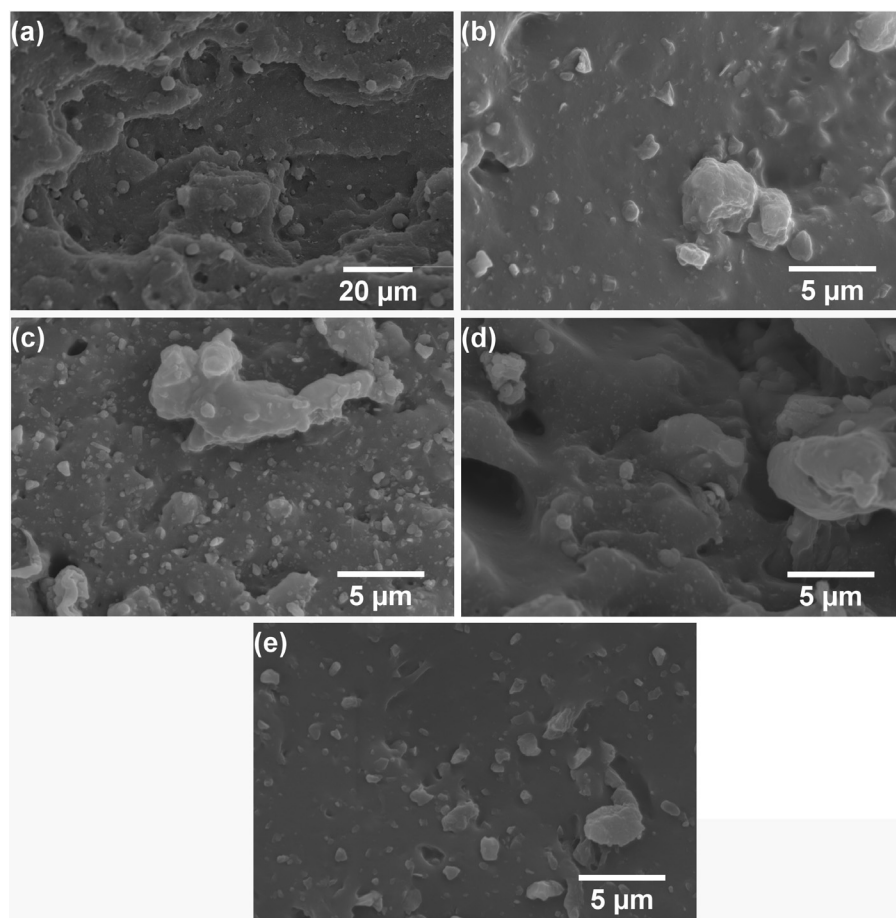


Fig. 6. SEM micrograph of hevea rubber nano composites with (a) 35 phr carbon black; (b) 35 phr carbon fly ash; (c) 35 phr eggshells; (d) 20 phr guayule bagasse; (e) 35 phr processing tomato peels.

contours, while GB had rod-like particles. ES particles had the highest particle density among the waste-derived fillers, while GB had the lowest. Filler loading in the composites was measured based on weight of the materials, therefore, substantially larger volumes of material were needed for the preparation of the composites with lower density (Table 2) for similar weight loadings.

3.2. Composites mechanical properties

Considerable enhancement of vulcanized rubber mechanical properties were obtained at all loadings for most of the waste-derived fillers (Fig. 3). The addition of waste-derived fillers, alone or in combination with CB, increased tensile strength of hevea from 9.96 MPa (unfilled) up to 29.38 MPa and tensile strength of unfilled guayule from 7.07 MPa (unfilled) up to 24.72 MPa (Fig. 3). Modulus (at 300% elongation) of unfilled compounds was also significantly increased with the addition of the different waste-derived fillers. In general, as the amount of waste-derived nano filler was increased above 5 phr, a decrease in 300% modulus was observed (Fig. 3). However, despite the gradual softening of the composite observed as the amount of carbon black filler was decreased, represented by a decreased of the slope in the stress versus strain curves (Figs. 4 and 5), higher values of 300% modulus than those of unfilled vulcanizates were achieved at all loadings of nano-sized waste-derived fillers, including composites containing only 35 phr of waste-derived fillers, for both guayule and hevea rubber (Fig. 3). It is also important to note the differences in stress versus strain behavior between guayule and hevea composites containing the same loadings of a specific waste-derived nano fillers (Figs. 4 and 5).

Most of the composites manufactured by partial replacement of carbon black with 5 phr to 20 phr of nano-sized ES, CFA and TP had very similar values of elongation at break to unfilled vulcanizates for

both rubbers used (Fig. 3). Significantly higher values of elongation at break to those of unfilled rubber were obtained at 35 phr of ES for both guayule and hevea nanocomposites. Tear strength of all waste-derived fillers/hevea composites was 0.21–1.82 times higher than tear strength of unfilled hevea compounds (Fig. 3), except for composites made with 20 phr of TP (with 15 phr of CB). Likewise, tear strength of all waste-derived fillers/guayule composites was 0.4–1.31 times higher than tear strength of unfilled guayule compounds (Fig. 3), except the composite containing 20 phr of GB (with 15 phr of CB).

Based on the four properties measured, reinforcement comparable to that of CB alone was obtained by partial replacement of CB with low loading (5 and 10 phr) of nano ES, TP and CFA (Fig. 3). Nano-ES particles showed outstanding reinforcing potential among the waste-derived fillers used, particularly for guayule rubber composites. Guayule composites containing 5 phr of nano-sized ES had significantly higher tensile strength than CB composites, with similar 300% modulus, elongation at break and tear strength. Furthermore, there was no significant difference between the tensile strength of guayule composites manufactured with 10, 20 and 35 phr of nano-ES particles and guayule composites made solely with CB. Hevea composites containing 10 phr nano-ES (with 25 phr of CB) had the highest tensile strength (29.38 MPa) among hevea composites containing waste-derived fillers, only 14% lower than CB composites (Fig. 3), but lower 300% modulus and tear strength compared to hevea composites made with 5 phr of TP and CFA. In general, hevea composites containing 5 phr of TP and CFA had the highest overall values of tensile, tear strength and 300% modulus among hevea composites containing waste-derived fillers.

Due to the low bulk density of GB, large volumes of material are required for 35 phr composites. It was impossible to prepare a master batch containing this amount of GB.

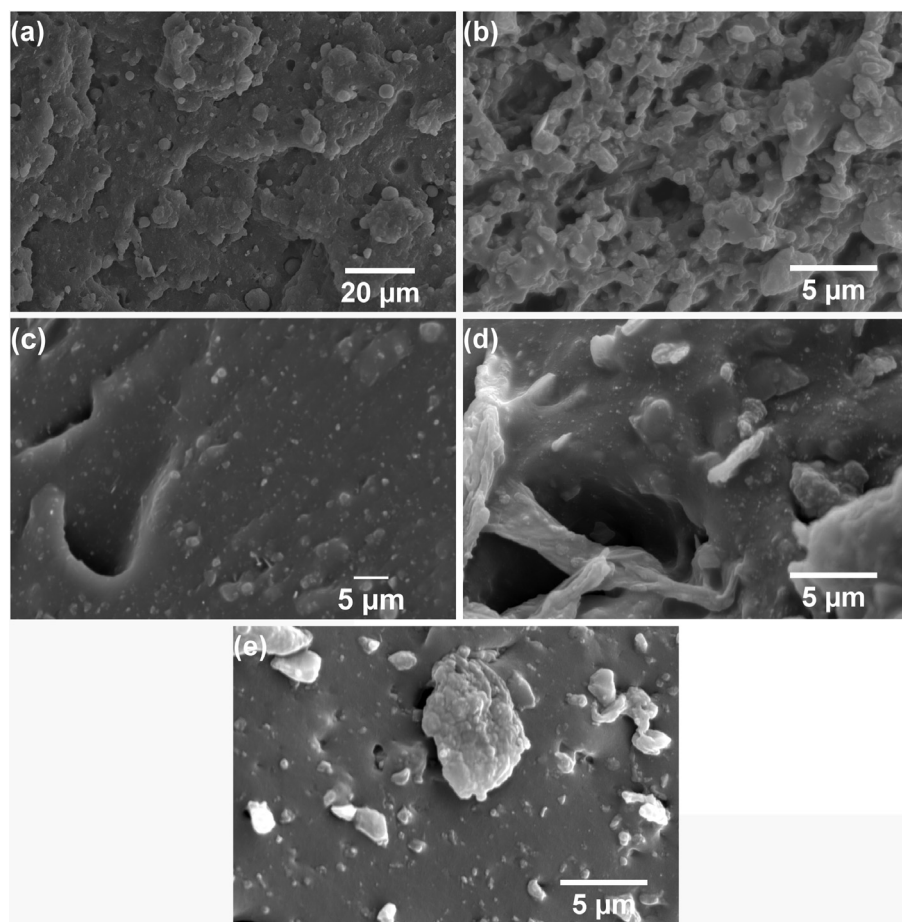


Fig. 7. SEM micrograph of guayule rubber nano composites with (a) 35 phr carbon black; (b) 35 phr carbon fly ash; (c) 35 phr eggshells; (d) 20 phr guayule bagasse; (e) 35 phr processing tomato peels.

3.3. Composites morphology

Scanning electron microscopy (SEM) of composite fracture surfaces revealed different composite morphology resulting from differences between the NRs and their interfacial interaction with the waste-derived fillers (Figs. 6 and 7). Both hevea and guayule rubber composites made with 35 phr CB had micro scale particles in the fracture surface (Figs. 6 a and 7 a), which are most likely aggregates of CB or compounding ingredients. In general, greater surface roughness was observed in guayule composites than hevea composites, due to a more ductile fracture of guayule.

In general, even distribution of the waste-derived fillers throughout both NRs was achieved at all loadings including 35 phr, but there was some agglomeration of the nano particles (Figs. 6 and 7) (SEM of composites at lower loadings of waste-derived fillers are not shown). Nevertheless, upon fracture, most of the particles remained embedded in both types of rubber.

Problems with uneven drying of master batches containing nano-sized CFA and GB particles were revealed by SEM. Composites made with these two fillers had a high prevalence of voids that probably resulted from the exit of residual water during curing of the materials. This problem was more obvious in guayule than hevea composites. Despite the presence of voids in CFA composites, most of the particles remained embedded in the rubbers (Figs. 6 b and 7 b). GB nanoparticles were hardly distinguishable in hevea composites (Fig. 6d), but bundles of the particles were observed intertwined within the guayule rubber (Fig. 7d).

3.4. Swelling behavior

Rapid toluene uptake was observed during the first 4 h of immersion

of the samples, followed by a decrease of sorption rate until the samples reached swelling equilibrium both for guayule and hevea composites (Fig. 8) (swelling curves of composites containing 10 and 20 phr of waste-derived fillers are not shown). In general, guayule composites had a higher swelling ratio and lower crosslink density than hevea composites containing equal filler loading (Table 3).

Composites containing low loadings of waste-derived filler had similar swelling behavior to CB composites. As the amount of the CB in the composites was decreased, swelling of the materials increased and crosslink density decreased. However, even at complete replacement of CB, composites made with ES and TP had more similar swelling behavior to CB composites than composites containing CFA and GB, particularly for the hevea composites (Fig. 8, Table 3).

3.5. Cluster analysis

Cluster analysis of composite mechanical properties led to classification of the composites into four groups with different characteristics for hevea composites and three groups for guayule composites (Fig. 9). Composites with the highest tensile and tear strength, high 300% modulus and elongation at break were grouped in cluster 2 for hevea composites and cluster 3 for guayule composites. These clusters included composites made with 35 phr with CB, 5 and 10 phr of waste-derived nano-sized fillers, except composites made with 10 phr of GB, which were classified into a different group of composites.

Hevea composites in cluster 1 (Fig. 9a) and guayule composites in cluster 2 (Fig. 9b) possessed high tensile strength and elongation at break, but medium values of tear strength and low 300% modulus. These clusters mainly grouped composites made with 20 phr and 35 phr of ES and 20 phr of CFA.

Unfilled compounds, composites made with 35 phr of TP and CFA,

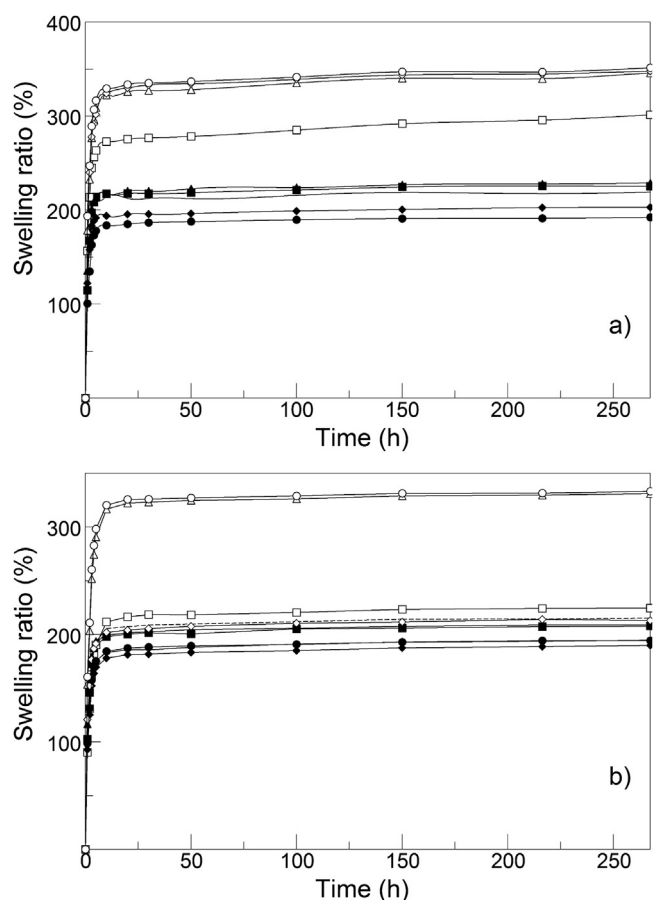


Fig. 8. Natural rubber nano composites swelling behavior. (a) Guayule rubber composites, (b) hevea rubber composites. Unfilled —○—, carbon black —●—, carbon fly ash 5phr —▲—, carbon fly ash 35phr —△—, eggshells 5phr —■—, eggshells 35phr —□—, guayule bagasse 5phr —◆—, guayule bagasse 20phr —◇—, processing tomato peels 5phr —■—, processing tomato peels 35phr —□—.

and composites containing 10 phr and 20 phr of nano-sized GB, were gathered in cluster 4 for hevea composites and cluster 1 for guayule composites. These composites had lower overall performance properties compared to previously described clusters both for hevea and guayule composites. Finally, hevea composites manufactured with 20 phr of TP had the lowest tensile strength, elongation at break and tear strength, but high modulus, and were grouped in cluster 3 (Fig. 9a).

3.6. Power consumption during mixing

The power required for the compounding of hevea and guayule rubber with different nano-sized waste-derived fillers and CB was compared to power consumption during mixing of macro and micro sized composites at equal filler loadings (Figs. 10 and S.1–S.7). Due to the lower bulk viscosity of guayule rubber (Schloman, 2005), mixing identical formulations required higher power for hevea than for guayule rubber compounds (Table 4).

Fillers were added to the rubber during the second step in the mixing protocol. As can be seen in guayule composites made with CFA (Fig. 10), partial and full replacement of CB with waste-derived filler reduced the power required in this step (panel 2 from left to right Fig. 10), even when nano-sized waste-derived filler particles were used. In general, upon addition of the filler, a progressive increase in power consumption was observed as the ratio of CB:waste-derived filler loading increased for both types of rubber (S.1–S.7). However, this trend was clearer in guayule than hevea composites.

Power consumption increased during the second step in the mixing procedure (panel 2 from left to right Figs. 10 and S.1–S.7), as the

Table 3

Swelling ratio at equilibrium and crosslink density (v_c) of natural rubber nano composites.

Rubber	Sample ^a	Swelling ratio at equilibrium (%)	v_c (10^{-3} mol/cm ³)
Guayule	Unfilled compound (no filler)	351.41	0.365
Guayule	35 phr carbon black	192.22	1.243
Guayule	5 phr tomato peel	225.26	0.899
Guayule	10 phr tomato peel	240.36	0.787
Guayule	20 phr tomato peel	276.75	0.591
Guayule	35 phr tomato peel	301.37	0.497
Guayule	5 phr eggshell	219.18	0.95
Guayule	10 phr eggshell	230.86	0.855
Guayule	20 phr eggshell	237.87	0.804
Guayule	5 phr carbon fly ash	228.79	0.871
Guayule	10 phr carbon fly ash	243.66	0.766
Guayule	20 phr carbon fly ash	287.15	0.548
Guayule	35 phr carbon fly ash	345.94	0.376
Guayule	5 phr guayule bagasse	202.94	1.112
Guayule	10 phr guayule bagasse	217.34	0.967
Guayule	20 phr guayule bagasse	348.06	0.372
Hevea	Unfilled compound (no filler)	333.2	0.41
Hevea	35 phr carbon black	194.36	1.228
Hevea	5 phr tomato peel	207.8	1.071
Hevea	10 phr tomato peel	211.76	1.03
Hevea	20 phr tomato peel	173.58	1.548
Hevea	35 phr tomato peel	224.49	0.914
Hevea	5 phr eggshell	194.79	1.222
Hevea	10 phr eggshell	191.63	1.264
Hevea	20 phr eggshell	182.97	1.389
Hevea	35 phr eggshell	215.21	0.997
Hevea	5 phr carbon fly ash	208.94	1.059
Hevea	10 phr carbon fly ash	224.44	0.915
Hevea	20 phr carbon fly ash	257.08	0.693
Hevea	35 phr carbon fly ash	331.1	0.415
Hevea	5 phr guayule bagasse	189.87	1.288
Hevea	10 phr guayule bagasse	251.58	0.725
Hevea	20 phr guayule bagasse	212.93	1.019

^a Total amount of filler (carbon black plus waste-derived filler), in all samples except unfilled compound, was 35 phr.

particle size of the waste-derived fillers in the composite decreased. However, this trend was not as clear as the effect of the change in ratio of CB:waste-derived filler loading. It was clearest for composites containing 35 phr of waste-derived fillers.

In the last step of the mixing protocol (panel 3 from left to right Fig. 10), the presence of CB in the formulation was the main factor affecting the power consumption. As the amount of CB in the compound increased, power consumption also increased for most of the formulations. However, for hevea composites, power consumption of compounds containing waste-derived fillers was very close to that of compounds containing CB alone (S.1–S.4). The minor substitution of only 5 phr CB with waste-derived fillers, reduced power consumption by 0.9%–10.5% in hevea composites and 0.8–19.7% in guayule composites, with the greatest power savings achieved with ES and GB in hevea and CFA and ES in guayule.

4. Discussion

Reinforcement of guayule and hevea NR achieved by nano-sized waste-derived fillers can be attributed to different factors, including high surface area offered by nano-sized particles which have higher surface area than bigger particles such as micro or macro sized particles, and good dispersion of these small particles as depicted by SEMs of surface fracture (Figs. 6 and 7). The high surface area of the nano-sized particles combined with uniform distribution throughout the material,

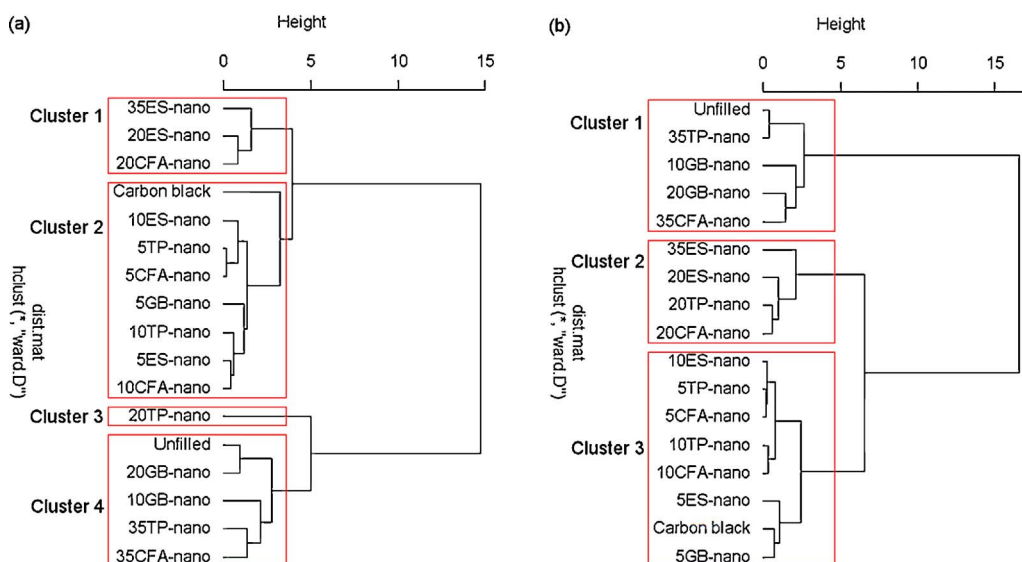


Fig. 9. Dendrograms obtained from hierarchical cluster analysis of (a) hevea and (b) guayule rubber formulations. Composite labels represent the amount of waste-derived filler in the sample, filler type and particle size. Total amount of filler (carbon black plus waste-derived filler), in all samples was 35 phr. Filler type: carbon fly ash (CFA), guayule bagasse (GB), eggshells (ES), processing tomato peels (TP).

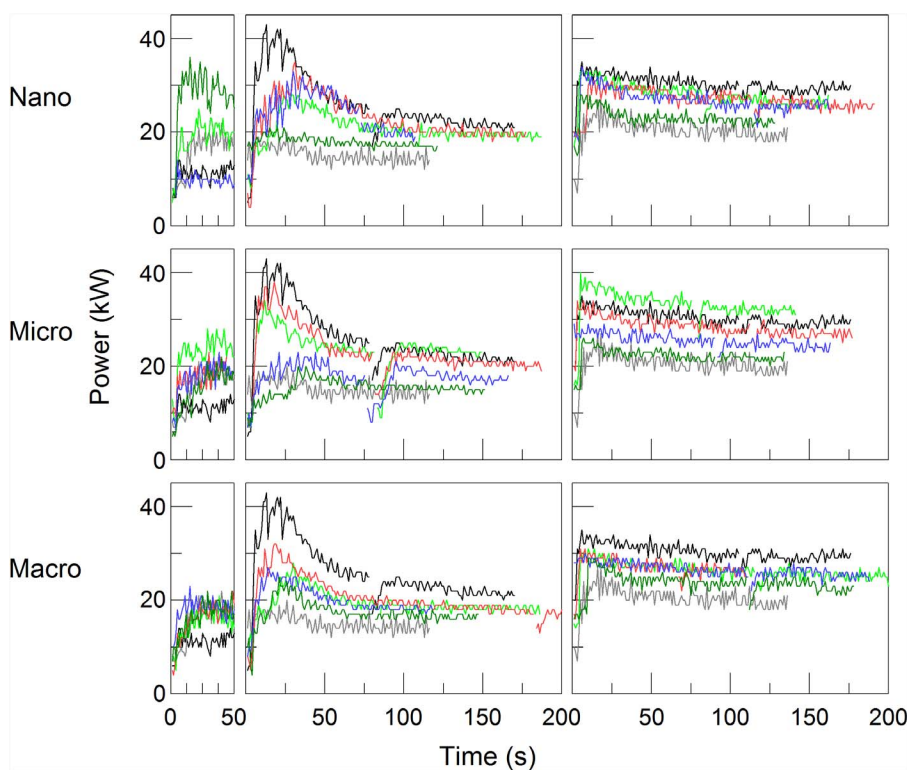


Fig. 10. Power consumption during mixing of guayule rubber composites manufactured using different size of carbon fly ash. Unfilled compound (gray), 35 phr carbon black composite (black), 5 phr waste filler composite (light green), 10 phr waste filler composite (red), 20 phr waste filler composite (blue), 35 phr waste filler composite (dark green). Total amount of filler (carbon black plus waste-derived filler), in all composites was 35 phr. Panels represent the steps in the mixing protocol. (For interpretation of the references to colour in this figure legend, the reader is referred to the web version of this article.)

allowed sufficient contact between the fillers and the polymers to limit chain movement, which results in increased polymer resistance to deformation and molecular separation, which can lead to failure (Hamed, 2000; Samsuri, 2013). This is reflected in the increased tear and tensile strength of composites compared to unfilled vulcanizates (Fig. 3).

Filler-filler networks and polymer-filler interactions are likely also to make significant contributions to the reinforcement (Figs. 6 and 7) especially for the guayule rubber composites, as has been indicated in macro and micro composites (Barrera and Cornish, 2015, 2016). The formation of a filler network within the rubber can considerably enhance mechanical properties (Bandyopadhyay-Ghosh et al., 2015; Samsuri, 2013) by interlocking the rubber chains within the filler network. Such filler networks are very strong with the waste-derived fillers under investigation because of their chemical composition and structural configurations that favor specific type of interactions such as

hydrogen bonds and ionic bonds between the particles. In previous work, specific interactions were found to be stronger in all the waste-derived fillers studied than in CB particles which interact by dispersive forces (Barrera et al., 2017). By using co-filler systems, in this case CB with waste-derived fillers at low loadings, the greater strength of waste-derived filler networks complements the CB-mediated reinforcement. Hence composites retained or even enhanced mechanical properties obtained with CB alone (Fig. 3). These synergistic effects were more pronounced in guayule than hevea rubber (Fig. 3), due to differences in rubber structure and composition (non-rubber components). Hevea rubber is a branched macromolecule while guayule has a more linear chain structure (Rensch et al., 1986), which allows it to flow more easily into the filler network. Furthermore, non-rubber components such as resins in guayule rubber that are not present in hevea rubber could act as compatibilizers between the rubber and the fillers.

Table 4
Power Consumption during Mixing of natural rubber composites.

Rubber	Filler	Average power (kW/s)
Guayule	Unfilled compound	17.93
Hevea	Unfilled compound	26.29
Guayule	35 phr carbon black	28.11
Hevea	35 phr carbon black	36.42

Rubber	Filler	Particle size	5phr*	10phr*	20phr*	35phr
Guayule	Guayule bagasse	macro	23.60	27.34	26.29	24.40
Guayule	Guayule bagasse	micro	25.31	24.87	21.47	–
Guayule	Guayule bagasse	nano	23.03	20.53	17.98	–
Guayule	Carbon fly ash	macro	22.91	22.73	23.99	20.81
Guayule	Carbon fly ash	micro	28.21	25.65	21.51	18.53
Guayule	Carbon fly ash	nano	24.11	24.94	25.67	20.56
Guayule	Eggshells	macro	22.88	22.35	21.06	19.94
Guayule	Eggshells	micro	27.85	24.76	22.69	20.47
Guayule	Eggshells	nano	25.92	26.13	20.21	20.83
Guayule	Tomato peels	macro	24.11	26.27	26.50	22.72
Guayule	Tomato peels	micro	23.08	25.62	–	–
Guayule	Tomato peels	nano	23.92	24.07	22.13	16.86
Hevea	Guayule bagasse	macro	34.64	34.98	32.18	31.22
Hevea	Guayule bagasse	micro	34.29	35.93	32.50	–
Hevea	Guayule bagasse	nano	28.67	29.98	20.24	–
Hevea	Carbon fly ash	macro	34.21	34.18	33.94	30.44
Hevea	Carbon fly ash	micro	36.32	34.94	30.77	32.50
Hevea	Carbon fly ash	nano	36.14	34.05	35.35	36.81
Hevea	Eggshells	macro	34.99	34.96	32.74	30.18
Hevea	Eggshells	micro	34.59	34.76	32.72	29.00
Hevea	Eggshells	nano	32.77	34.14	33.48	31.32
Hevea	Tomato peels	macro	34.35	35.05	35.51	33.43
Hevea	Tomato peels	micro	33.01	34.54	–	–
Hevea	Tomato peels	nano	34.90	33.48	34.61	33.68

* Total amount of filler (carbon black plus waste-derived filler), in all samples was 35 phr.

Despite the contribution of filler networks in the reinforcement of the polymers, polymer–filler interaction represents a stronger

reinforcement mechanism. CB possesses a non-polar surface more compatible with non-polar poly-isoprene chains in NR than the more polar waste-derived fillers (Barrera et al., 2017; Leblanc, 2002), thus stronger polymer–filler interaction. Adsorption of rubber into the CB surface acts as additional crosslinks (Chenal et al., 2007), which translates to stronger materials. At high loadings of waste-derived filler, reinforcement achieved through filler–filler interaction is not comparable to the reinforcement obtained from polymer–filler interactions between CB and NR (Barrera and Cornish, 2016; Jong, 2014), hence a decrease in properties is observed (Fig. 3). However, some of the waste-derived fillers, namely ES and TP, retained high values of tensile and tear strength at loadings as high as 35 phr for guayule composites and 10 phr for hevea composites (Fig. 3). This indicates differences in the strength of polymer–filler interaction among the waste-derived fillers due to differences in chemical and structural composition of the filler. These differences were also observed as differences in surface energy of the materials in previous studies (Barrera et al., 2017).

Overall contribution of filler–filler networks and polymer–filler interactions among the different fillers was also evinced by the difference in crosslink density determined through swelling of the composites (Table 3). Composites made with low loading of waste-derived filler, particularly ES and TP, had the highest crosslink density. Solvent absorption measurements yield an apparent crosslink density that can be explained by the sum of both chemical and physical crosslinks, such as entanglement of polymer chains within the filler network and adsorption of rubber to the surface of the filler (Lee et al., 1994).

Despite their lower particle size, nano-sized waste-derived fillers did not improve mechanical properties much beyond the micro-sized particles previously studied (Barrera and Cornish, 2016, 2015) (Figs. 11 and 12). In general, composites containing micro-sized waste-derived fillers as co-fillers with CB performed as well or better than composites containing equivalent combination with nano-sized waste-derived fillers. Furthermore, mixing of high loadings micro-sized particles into compounds required less power than nano-sized particles (Table 4).

The similar or lower reinforcement and the higher power consumption of nano-sized waste-derived filler composites, compared to

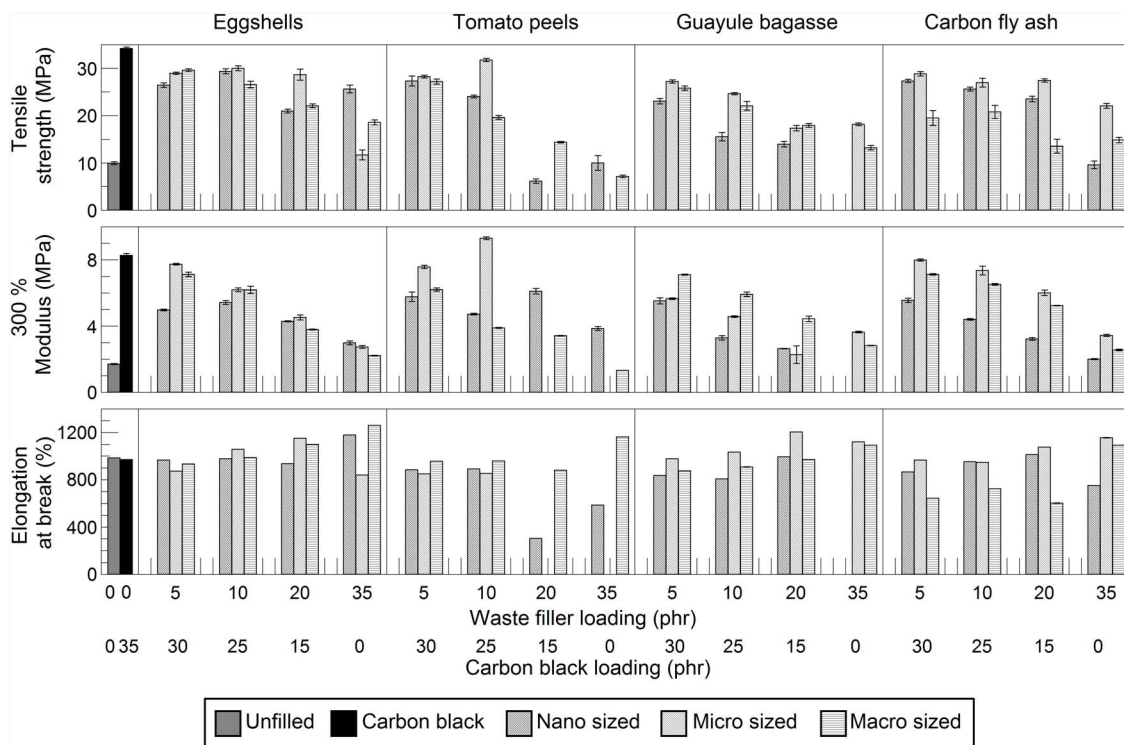


Fig. 11. Mechanical properties of hevea rubber composites manufactured using various particle size particles obtained from different waste derived materials. Total amount of filler (carbon black plus waste-derived filler), in all composites was 35 phr. As the waste filler loading increases the carbon black filler decreases by the same weight amount.

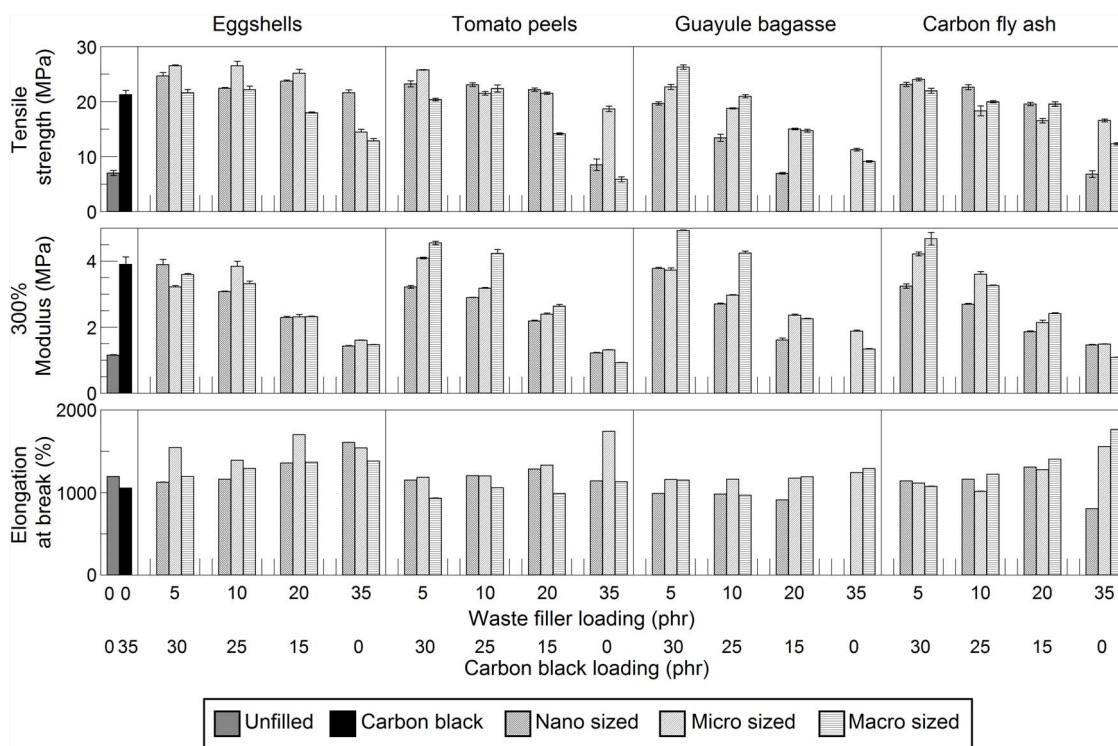


Fig. 12. Mechanical properties of guayule rubber composites manufactured using various particle size particles obtained from different waste derived materials. Total amount of filler (carbon black plus waste-derived filler), in all composites was 35 phr. As the waste filler loading increases the carbon black filler decreases by the same weight amount.

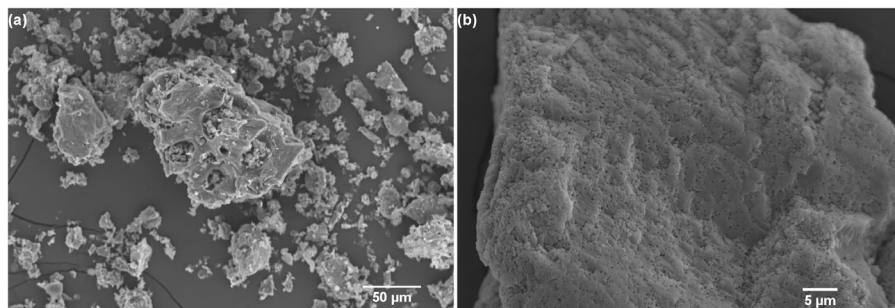


Fig. 13. SEM micrographs of waste-derived filler particles. (a) Carbon fly ash; (b) eggshells.

micro-composites, are due to increased attraction between the particles caused by their smaller size. Exposure of polar functional groups, changes in crystallinity and increases in surface area that result from mechanical and/or chemical treatment (Gamble et al., 2012; Paul et al., 2007) increase the interaction between waste-derived filler particles. Despite the dispersion method used, agglomerates of the nano-sized waste-derived fillers may form during drying due to this strong inter-particle interaction. This would result in lower final particle surface area and increase the energy required for uniform dispersion in the compound.

Other factors that influenced the mechanical properties and processability of hevea and guayule composites include hydrodynamic effects, particle structure, particle size distribution, filler alkalinity and reactivity with curing chemicals (Barrera and Cornish, 2016, 2015). Inclusion of a non-deformable phase to the elastomer contributes particularly to the enhancement of the modulus (Fröhlich et al., 2005; Roland, 2016). The hydrodynamic effect has been described as a function of the volume fraction of the filler and shape factor (Payne, 1962). GB has both the lowest particle density among the waste-derived fillers as well as the highest aspect ratio (length to width ratio) (Table 2). Therefore, GB composites had potentially a large contribution of hydrodynamic reinforcement because substantially larger volumes of material were needed for the preparation of the composites of

similar weight loadings. Nevertheless, better reinforcement was obtained by the other waste-derived fillers which indicate stronger contribution from other reinforcing mechanisms, beyond hydrodynamic effects of the waste-derived particles. Furthermore, larger number of particles confined in the composites favor interaction between the particles, which may lead to agglomeration of the filler and result in poor reinforcement.

Waste-derived fillers like ES and CFA possess unique and complex porous structures at the micro-scale (Fig. 13), that increase effective surface area and contribute to the observed reinforcement (Barrera and Cornish, 2016). These structural features may be lost at the nano-scale. Broad particle size distribution of micro fillers allows better packing of the particles in the rubber, which generates compounds with lower viscosity than nano composites. Furthermore, high compound viscosity is obtained with the addition of highly branched aggregate structures of nano-sized particles (Gerspacher and Wampler, 2001; Khan and Bhat, 2014). Hence higher power was required to mix into the rubber CB and nano-sized waste-derived fillers compared to larger filler. Also, the presence of terpene resins, such as those in GB, can act as plasticizers, which would increase ductility of the materials (Barrera and Cornish, 2015).

Given that curing conditions were the same for all the composites, pH and active surface of waste-derived fillers resulted in different

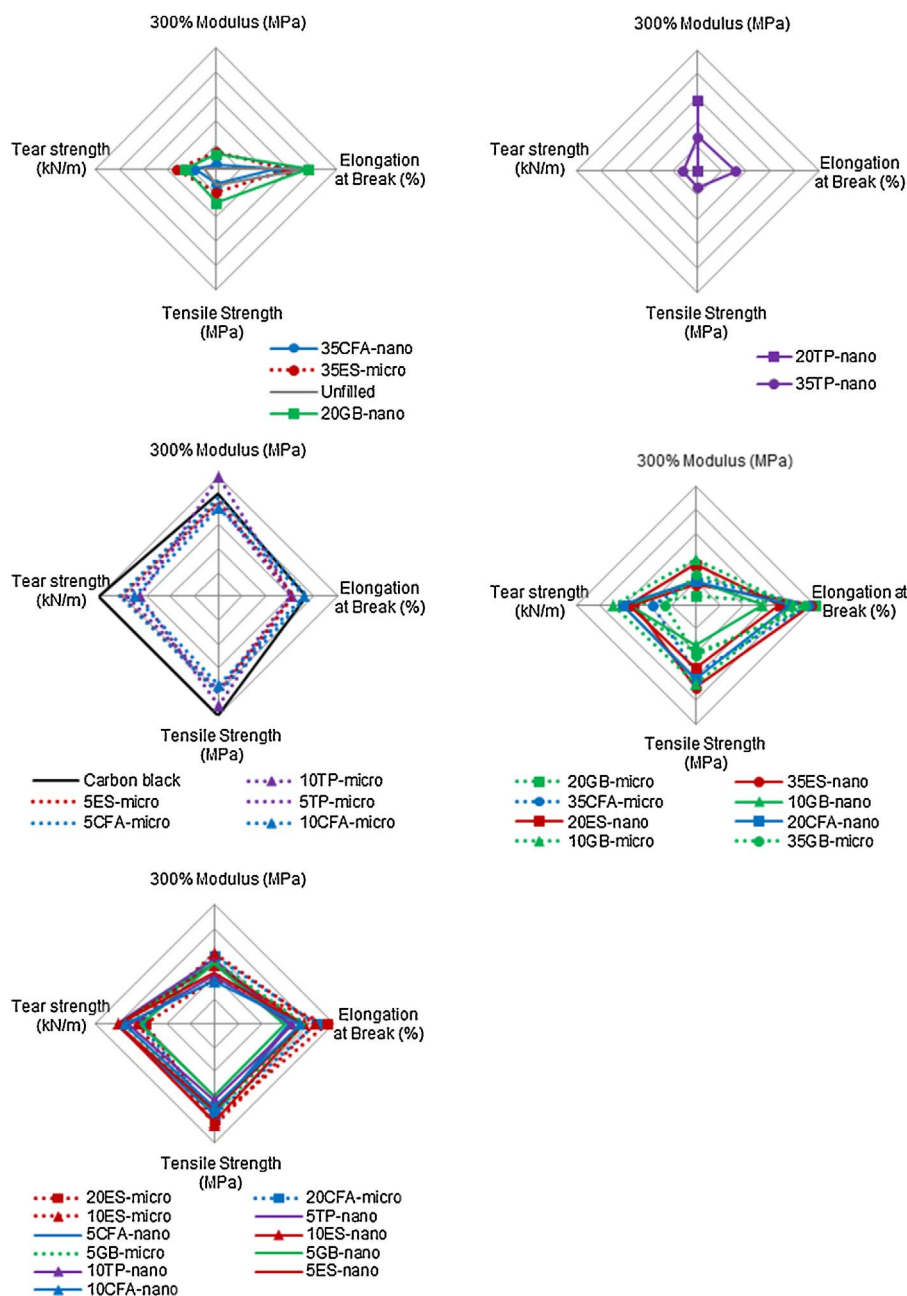


Fig. 14. Radar chart representing mechanical properties of hevea composites made with nano and micro size waste-derived fillers. Composite labels represent the amount of waste-derived filler in the sample, filler type and particle size. Total amount of filler (carbon black plus waste-derived filler), in all samples was 35 phr. Filler type: carbon fly ash (CFA), guayule bagasse (GB), eggshells (ES), processing tomato peels (TP).

performance properties particularly for guayule due to its slower curing rate than hevea. Alkaline fillers like ES can cause faster curing rates and increased crosslink density which can improve modulus, tensile and tear strength (Barrera and Cornish, 2016; Byers, 2001). In contrast, the silanol groups found in CFA can react with the compounding ingredients and decrease the curing rate of the compound (Byers, 2001). Optimal curing conditions for the different composites have not yet been determined.

Although composites manufactured with GB required low mixing power, overall mechanical properties of composites containing loadings greater than 5 phr of GB were lower than other waste-derived fillers used. Furthermore, the amount of GB that could be incorporated into the master batch was limited, due to the low density of this material, which required higher volume fractions to obtain the same weight loadings. Currently there are other alternatives to generate added-value products from this residue such as the production of bio-oil through pyrolysis of the material (Boateng et al., 2009, 2010). Composites manufactured with nano-sized GB and CFA also had higher moisture

retention than ES or TP, due to their hydrophilic nature.

Different combinations of composite properties achieved with these co-filler systems are not usually achieved with a single conventional reinforcing filler (Fig. 14 and 15). Enhancement of NR tensile strength by CB, for instance, is generally paired with a decrease in flexibility of the material. Composites with higher flexibility at comparable strength were obtained with some of the waste-derived fillers used. In addition, decreases in power consumption were obtained even with the replacement of a small fraction of CB in the composite. This could really benefit the economics and sustainability of large scale rubber product manufacture.

Many researchers have focused on biobased nano-sized particles due to the inherent benefits of large surface area of the particles and lower carbon foot print (Angellier et al., 2005a; Bitinis et al., 2013; Bras et al., 2010; Visakh et al., 2012). However, commercial application of these nano fillers is restricted by their limited availability, high production cost and strong tendency to agglomerate (Abraham et al., 2011; Angellier et al., 2005b; Szeluga et al., 2015). The partial replacement of

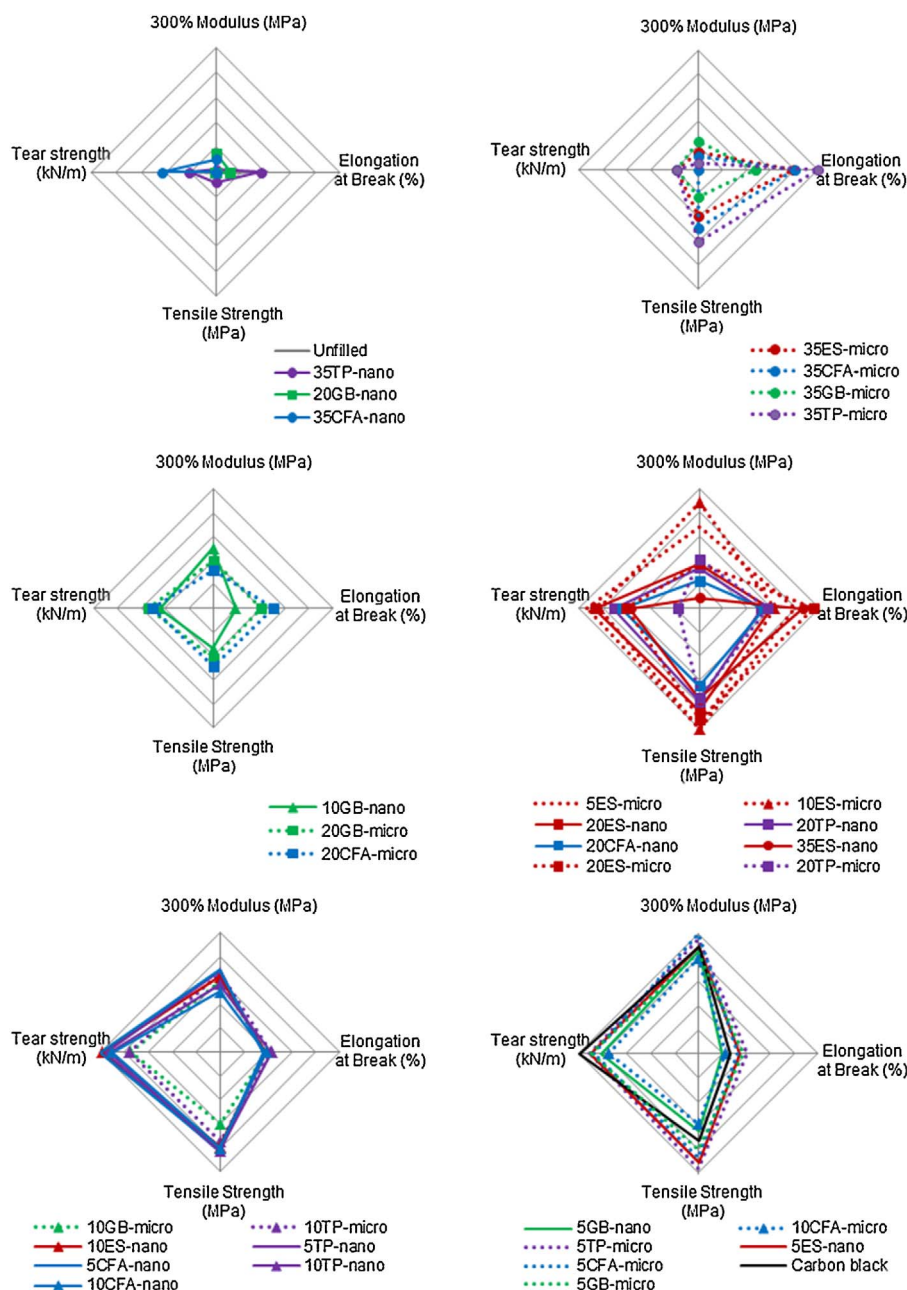


Fig. 15. Radar chart representing mechanical properties of guayule composites made with nano and micro size waste-derived fillers. Composite labels represent the amount of waste-derived filler in the sample, filler type and particle size. Total amount of filler (carbon black plus waste-derived filler), in all samples was 35 phr. Filler type: carbon fly ash (CFA), guayule bagasse (GB), eggshells (ES), processing tomato peels (TP).

CB with micro-sized waste-derived fillers, which can be made at a lower cost than nano-sized particles, without loss of mechanical properties, suggests a potential added-value for these highly abundant materials.

5. Conclusion

Partial replacement of CB with waste-derived fillers can generate material with performance characteristics suitable for commercial applications while adding value to agro-industrial residues and offering low cost and sustainable alternative source of fillers for NR products. Such fillers would supplement increasing demand for fillers and mitigate projected shortages. Positive impacts on overall manufacturing costs of rubber products may be achieved through the use of micro sized fillers that can be cheaply made and also decrease power consumption during rubber compounding. Furthermore, optimization of curing profiles for each rubber and surface modification of the fillers may result in materials with properties superior to those so far achieved.

Acknowledgments

We thank Ohio Third Frontier, Ohio Research Scholars Program in Technology-Enabling and Emergent Materials (TECH 09-026), Institute for Materials Research Facility Grant, The Ohio State University and USDA National Institute of Food and Agriculture (Hatch project 230837) for providing financial support for this project. We also thank the Fulbright for sponsoring Cindy Barrera during her Ph.D. program, and Dr. Frederick C. Michel Jr. and Arisdyne systems for allowing us to use their particle size analyzer and ultrasonic processor.

Appendix A. Supplementary data

Supplementary data associated with this article can be found, in the online version, at doi:<http://dx.doi.org/10.1016/j.indcrop.2017.05.045>.

References

- ASTM International, 2012. ASTM Standard D624-00. Standard Test Method for Tear Strength of Conventional Vulcanized Rubber and Thermoplastic Elastomers. <http://dx.doi.org/10.1520/D0624-00R12>.
- ASTM International, 2013a. ASTM Standard D412 - 15a. Standard Test Methods for Vulcanized Rubber and Thermoplastic Elastomers—Tension. <http://dx.doi.org/10.1520/D0412-15A>.
- ASTM International, 2013b. ASTM Standard D6814 - 02. Standard Test Method for Determination of Percent Devulcanization of Crumb Rubber Based on Crosslink Density. <http://dx.doi.org/10.1520/D6814-02R13>.
- Abraham, E., Deepa, B., Pothan, L.A., Jacob, M., Thomas, S., Cvelbar, U., Anandjiwala, R., 2011. Extraction of nanocellulose fibrils from lignocellulosic fibres: a novel approach. *Carbohydr. Polym.* 86, 1468–1475. <http://dx.doi.org/10.1016/j.carbpol.2011.06.034>.
- Abraham, E., Deepa, B., Pothan, L.A., John, M., Narine, S.S., Thomas, S., Anandjiwala, R., 2013. Physicochemical properties of nanocomposites based on cellulose nanofibre and natural rubber latex. *Cellulose* 20, 417–427. <http://dx.doi.org/10.1007/s10570-012-9830-1>.
- Angellier, H., Molina-Boisseau, S., Dufresne, A., 2005a. Mechanical properties of waxy maize starch nanocrystal reinforced natural rubber. *Macromolecules* 38, 9161–9170. <http://dx.doi.org/10.1021/ma0512399>.
- Angellier, H., Molina-Boisseau, S., Lebrun, L., Dufresne, A., 2005b. Processing and structural properties of waxy maize starch nanocrystals reinforced natural rubber. *Macromolecules* 38, 3783–3792. <http://dx.doi.org/10.1021/ma050054z>.
- Bandyopadhyay-Ghosh, S., Ghosh, S.B., Sain, M., 2015. The use of biobased nanofibres in composites. In: Faruk, O., Sain, M. (Eds.), *Biofiber Reinforcements in Composite Materials*. Elsevier, Sawston, Cambridge, pp. 571–647. <http://dx.doi.org/10.1533/9781782421276.5.571>.
- Barrera, C.S., Cornish, K., 2015. Novel mineral and organic materials from agro-Industrial residues as fillers for natural rubber. *J. Polym. Environ.* 23, 437–448. <http://dx.doi.org/10.1007/s10924-015-0737-4>.
- Barrera, C.S., Cornish, K., 2016. High performance waste-derived filler/carbon black reinforced guayule natural rubber composites. *Ind. Crops Prod.* 86, 132–142. <http://dx.doi.org/10.1016/j.indcrop.2016.03.021>.
- Barrera, C.S., Cornish, K., Soboyejo, A.B.O., 2017. Quantification of the contribution of filler characteristics to natural rubber reinforcement using principal component analysis. *Rubber Chem. Technol.* <http://dx.doi.org/10.5254/rct.82.83716>. (in press).
- Bitinis, N., Fortunati, E., Verdejo, R., Bras, J., Kenny, J.M., Torre, L., López-Manchado, M.A., 2013. Poly(lactic acid)/natural rubber/cellulose nanocrystal bionanocomposites. Part II: properties evaluation. *Carbohydr. Polym.* 96, 621–627. <http://dx.doi.org/10.1016/j.carbpol.2013.03.091>.
- Boateng, A.A., Mullen, C.A., Goldberg, N.M., Hicks, K.B., McMahan, C.M., Whalen, M.C., Cornish, K., 2009. Energy-dense liquid fuel intermediates by pyrolysis of guayule (*Parthenium argentatum*) shrub and bagasse. *Fuel* 88, 2207–2215. <http://dx.doi.org/10.1016/j.fuel.2009.05.023>.
- Boateng, A.A., Mullen, C.A., McMahan, C.M., Whalen, M.C., Cornish, K., 2010. Guayule (*Parthenium argentatum*) pyrolysis and analysis by PY-GC/MS. *J. Anal. Appl. Pyrolysis* 87, 14–23. <http://dx.doi.org/10.1016/j.jaap.2009.09.005>.
- Bras, J., Hassan, M.L., Bruzesse, C., Hassan, E.A., El-Wakil, N.A., Dufresne, A., 2010. Mechanical, barrier, and biodegradability properties of bagasse cellulose whiskers reinforced natural rubber nanocomposites. *Ind. Crops Prod.* 32, 627–633. <http://dx.doi.org/10.1016/j.indcrop.2010.07.018>.
- Byers, J.T., 2001. Filler–Non-black. In: Baranwal, K.C., Stephens, H.L. (Eds.), *Basic Elastomer Technology*. American Chemical society, Rubber division, Akron, Ohio, pp. 82–111.
- Chao, H., Riggelman, R.A., 2013. Effect of particle size and grafting density on the mechanical properties of polymer nanocomposites. *Polymer (Guildf)* 54, 5222–5229. <http://dx.doi.org/10.1016/j.polymer.2013.07.018>.
- Chenal, J.M., Gauthier, C., Chazeau, L., Guy, L., Bomal, Y., 2007. Parameters governing strain induced crystallization in filled natural rubber. *Polymer (Guildf)* 48, 6893–6901. <http://dx.doi.org/10.1016/j.polymer.2007.09.023>.
- Choi, S.S., Nah, C., Lee, S.G., Joo, C.W., 2003. Effect of filler–filler interaction on rheological behaviour of natural rubber compounds filled with both carbon black and silica. *Polym. Int.* 52, 23–28. <http://dx.doi.org/10.1002/pi.975>.
- Cordeiro, N., Gouveia, C., John, M.J., 2011. Investigation of surface properties of physico-chemically modified natural fibres using inverse gas chromatography. *Ind. Crops Prod.* 33, 108–115. <http://dx.doi.org/10.1016/j.indcrop.2010.09.008>.
- Cornish, K., 1996. Hypoallergenic natural rubber products from *Parthenium argentatum* (Gray) and other non-*hevea brasiliensis* species. U.S. Patent, No. 5,580,942.
- Donnet, J.B., Custodero, E., 2013. Reinforcement of elastomers by particulate fillers. In: Mark, J.E., Erman, B., Roland, M. (Eds.), *The Science and Technology of Rubber*. Elsevier, pp. 383–416. <http://dx.doi.org/10.1016/B978-0-12-394584-6.00008-X>.
- Fang, Q., Song, B., Tee, T.T., Sin, L.T., Hui, D., Bee, S.T., 2014. Investigation of dynamic characteristics of nano-size calcium carbonate added in natural rubber vulcanizate. *Compos. Part B Eng.* 60, 561–567. <http://dx.doi.org/10.1016/j.compositesb.2014.01.010>.
- Fröhlich, J., Niedermeier, W., Luginsland, H.D., 2005. The effect of filler–filler and filler–elastomer interaction on rubber reinforcement. *Compos. Part A Appl. Sci. Manuf.* 36, 449–460. <http://dx.doi.org/10.1016/j.compositesa.2004.10.004>.
- Gamble, J.F., Leane, M., Olusanmi, D., Tobyn, M., Supuk, E., Khoo, J., Naderi, M., 2012. Surface energy analysis as a tool to probe the surface energy characteristics of micronized materials – a comparison with inverse gas chromatography. *Int. J. Pharm.* 422, 238–244. <http://dx.doi.org/10.1016/j.ijpharm.2011.11.002>.
- Gerspacher, M., Wampler, W., 2001. Fillers – carbon black. In: Baranwal, K.C., Stephens, H. (Eds.), *Basic Elastomer Technology*. American Chemical society, Rubber division, Akron, Ohio, pp. 57–81.
- Gopalan Nair, K., Dufresne, A., 2003. Crab shell chitin whisker reinforced natural rubber nanocomposites. 1. Processing and swelling behavior. *Biomacromolecules* 4, 657–665. <http://dx.doi.org/10.1021/bm020127b>.
- Hamed, G.R., 2000. Reinforcement of rubber. *Rubber Chem. Technol.* 73, 524–533. <http://dx.doi.org/10.5254/1.3547603>.
- Intharapat, P., Kongnoo, A., Kateunggan, K., 2013. The potential of chicken eggshell waste as a bio-filler filled epoxidized natural rubber (ENR) composite and its properties. *J. Polym. Environ.* 21, 245–258. <http://dx.doi.org/10.1007/s10924-012-0475-9>.
- Ishak, Z.A.M., Bakar, A.A., 1995. An investigation on the potential of rice husk ash as fillers for epoxidized natural rubber (ENR). *Eur. Polym. J.* 31, 259–269.
- Jong, L., 2014. Modulus enhancement of natural rubber through the dispersion size reduction of protein/fiber aggregates. *Ind. Crops Prod.* 55, 25–32. <http://dx.doi.org/10.1016/j.indcrop.2014.01.057>.
- Kato, a., Kokubo, Y., Tsuchi, R., Ikeda, Y., 2014. Hydrophobic and hydrophilic silica-filled cross-linked natural rubber (NR): structure and properties. In: Kohjiya, S., Ikeda, Y. (Eds.), *Chemistry, Manufacture and Applications of Natural Rubber*. Elsevier, Sawston, Cambridge, pp. 193–215. <http://dx.doi.org/10.1533/9780857096913.1.193>.
- Khan, I., Bhat, A., 2014. Micro and nano calcium carbonate filled natural rubber composites and nanocomposites. In: Thomas, Sabu, Han, Chin, Chan, Laly, Pothan, Jithin, Joy, H.M. (Eds.), *Natural Rubber Materials. Composites and Nanocomposites*. The Royal Society of Chemistry, pp. 467–487. <http://dx.doi.org/10.1039/9781849737654-00467>.
- Kohls, D.J., Beaucage, G., 2002. Rational design of reinforced rubber. *Curr. Opin. Solid State Mater. Sci.* 6, 183–194. [http://dx.doi.org/10.1016/S1359-0286\(02\)00073-6](http://dx.doi.org/10.1016/S1359-0286(02)00073-6).
- Kueseng, K., Jacob, K.I., 2006. Natural rubber nanocomposites with SiC nanoparticles and carbon nanotubes. *Eur. Polym. J.* 42, 220–227. <http://dx.doi.org/10.1016/j.eurpolymj.2005.05.011>.
- Leblanc, J., 2002. Rubber–filler interactions and rheological properties in filled compounds. *Prog. Polym. Sci.* 27, 627–687. [http://dx.doi.org/10.1016/S0079-6700\(01\)00040-5](http://dx.doi.org/10.1016/S0079-6700(01)00040-5).
- Lee, S., Pawlowski, H., Coran, A.Y., 1994. Method for estimating the chemical crosslink densities of cured natural rubber and styrene-butadiene rubber. *Rubber Chem. Technol.* 67, 854–864. <http://dx.doi.org/10.5254/1.3538716>.
- Moore, M., 2015. Exec: Expect Carbon Black Shortage in Five Years.
- Murakami, K., Iio, S., Ikeda, Y., Ito, H., Tosaka, M., Kohjiya, S., 2003. Effect of silane-coupling agent on natural rubber filled with silica generated in situ. *J. Mater. Sci.* 38, 1447–1455. <http://dx.doi.org/10.1023/A:1022908211748>.
- Nardin, M., Balard, H., Papirer, E., 1990. Surface characteristics of commercial carbon fibres determined by inverse gas chromatography. *Carbon N. Y.* 28, 43–48. [http://dx.doi.org/10.1016/0008-6223\(90\)90091-C](http://dx.doi.org/10.1016/0008-6223(90)90091-C).
- Notch consulting Inc, 2015. Carbon black and silica in the tire markets challenges and opportunities. In: *Proceedings of the Tire Technology Expo*. Cologne, Germany.
- Pasquini, D., Teixeira, E.D.M., Curvelo, A.A.D.S., Belgacem, M.N., Dufresne, A., 2010. Extraction of cellulose whiskers from cassava bagasse and their applications as reinforcing agent in natural rubber. *Ind. Crops Prod.* 32, 486–490. <http://dx.doi.org/10.1016/j.indcrop.2010.06.022>.
- Paul, K.T., Satpathy, S.K., Manna, I., Chakraborty, K.K., Nando, G.B., 2007. Preparation and characterization of nano structured materials from fly ash: a waste from thermal power stations, by high energy ball milling. *Nanoscale Res. Lett.* 2, 397–404. <http://dx.doi.org/10.1007/s11671-007-9074-4>.
- Payne, A.R., 1962. The dynamic properties of carbon black loaded natural rubber vulcanizates. Part II. *J. Appl. Polym. Sci.* 6, 368–372. <http://dx.doi.org/10.1002/app.1962.070062115>.
- Pedini, S.K., Bosnyak, C.P., Henderson, N.M., Ellison, C.J., Paul, D.R., 2014. Nanocomposites from styrene-butadiene rubber (SBR) and multiwall carbon nanotubes (MWCNT) part 1: morphology and rheology. *Polym. (United Kingdom)* 55, 258–270. <http://dx.doi.org/10.1016/j.polymer.2013.11.003>.
- Pourriahi, S., 2016. Report: Uncertainty Looms over Carbon Black Market in Europe..
- R Core Team, 2014. *R: A Language and Environment for Statistical Computing*. R: A Language and Environment for Statistical Computing.
- Rattanasom, N., Saowapark, T., Deepasertkul, C., 2007. Reinforcement of natural rubber with silica/carbon black hybrid filler. *Polym. Test.* 26, 369–377. <http://dx.doi.org/10.1016/j.polymertesting.2006.12.003>.
- Rensch, G.J., Phillips, P.J., Vatansever, N., Gonzalez, V.A., 1986. The cis crystallization behavior of cis-polyisoprenes extracted from the guayule plant. *J. Polym. Sci. Part B Polym. Phys.* 24, 1943–1959. <http://dx.doi.org/10.1002/polb.1986.090240904>.
- Roland, C.M., 2016. Reinforcement of elastomers. *Ref. Modul. Mater. Sci. Mater. Eng.* 1–9. <http://dx.doi.org/10.1016/B978-0-12-803581-8.02163-9>.
- Samsuri, A. Bin, 2013. Theory and mechanisms of filler reinforcement in natural rubber. In: Thomas, Sabu, Chan, Chin Han, Pothan, Laly, Joy, Jithin, Maria, H. (Eds.), *Natural Rubber Materials: Volume 2: Composites and Nanocomposites*. The Royal Society of Chemistry, pp. 73–111. <http://dx.doi.org/10.1039/9781849737654-00073>.
- Schloman, W.W., 2005. Processing guayule for latex and bulk rubber. *Ind. Crops Prod.* 22, 41–47. <http://dx.doi.org/10.1016/j.indcrop.2004.04.031>.
- Sheehan, C., Bisio, A.L., 1966. Polymer/solvent interaction parameters. *Rubber Chem. Technol.* 39, 149–192. <http://dx.doi.org/10.5254/1.3544827>.
- Stöckelhuber, K.W., Das, A., Jurk, R., Heinrich, G., 2010. Contribution of physico-chemical properties of interfaces on dispersibility, adhesion and flocculation of filler particles in rubber. *Polymer (Guildf)* 51, 1954–1963. <http://dx.doi.org/10.1016/j.polymer.2010.03.013>.
- Szeluga, U., Kumanek, B., Trzebicka, B., 2015. Synergy in hybrid polymer/nanocarbon

- composites. A review. *Compos. Part A Appl. Sci. Manuf.* 73, 204–231. <http://dx.doi.org/10.1016/j.compositesa.2015.02.021>.
- Tohsan, A., Ikeda, Y., 2014. Generating particulate silica fillers *in situ* to improve the mechanical properties of natural rubber (NR). *Chemistry, Manufacture and Applications of Natural Rubber*. Elsevierpp. 168–192. <http://dx.doi.org/10.1533/9780857096913.1.168>.
- Visakh, P.M., Thomas, S., Oksman, K., Mathew, A.P., 2012. Crosslinked natural rubber nanocomposites reinforced with cellulose whiskers isolated from bamboo waste: processing and mechanical/thermal properties. *Compos. Part A Appl. Sci. Manuf.* 43, 735–741. <http://dx.doi.org/10.1016/j.compositesa.2011.12.015>.